

**OPTIMAL TRAJECTORY ANALYSIS OF HIGH ANGLE OF ATTACK MISSILES**

Mario Innocenti, Associate Professor, Associate Fellow AIAA  
 and  
 Francesco Nasuti, Doctoral Student

*Department of Electrical Systems and Automation  
 University of Pisa, 56126 Pisa Italy*

Introduction

The present work deals with the generation of a trajectory envelope during the midcourse phase of flight of a missile capable of achieving controllable maneuvering at angles of attack beyond stall. A sample scenario represented by a three dimensional heading reversal maneuver is considered and evaluated in detail. Trajectory analysis and synthesis are carried out using two approaches. The first approach is a traditional nonlinear optimization procedure, with the added capability of high angles of attack and non zero sideslip. The optimal trajectory is found by minimizing a performance index, that contains constraints on state and control variables, as well as a minimum time structure. This approach is also used to perform a sensitivity evaluation with respect to design parameters such as thrust to weight ratio.

A second approach is a direct optimization in the "agility" state space. Curvilinear coordinates are used to represent the missile motion in space, and a performance index is minimized, which contains parameters like torsion and curvature.

The present paper describes the initial development of the optimization algorithm and contains preliminary results, which must be intended as validation of the optimal control strategy. Resulting time histories of differential geometry parameters are also available. The graphical results are presented using the Matlab™ computational environment.

The Flight Vehicle Model

The baseline flight vehicle model considered herein is representative of a generic air-air missile taken from<sup>(1)</sup>.

*"Copyright© 1996 by Mario Innocenti and Francesco Nasuti. Published by the American Institute of Aeronautics and Astronautics, Inc. and the International Council of Aeronautical Sciences, with permission."*

Due to the preliminary phase of trajectory analysis, several approximations were made on the dynamic characteristics of the system for the purpose of keeping the model as simple as possible, and because of the absence of accurate aerodynamic data. As a better aerodynamics becomes available, the model will be modified accordingly.

The optimal trajectory is computed with respect of a set of inputs given by angle of attack, sideslip angle, and main thrust ( $\alpha, \beta, T$ ), the presence of reaction jets is not explicitly included at the present time. A point mass model is used, assuming therefore that the attitude time constant is much smaller compared to the trajectory motion. In order to reduce instantaneous changes of the control angle, as a result of point mass optimization, the angle of attack and sideslip angles are governed by a first order dynamics, representative of the missile short period characteristics. During the maneuver, the total mass is assumed to remain constant and the force contribution due to reaction jets is neglected.

The reference systems used are standard for this type of application and they are described<sup>(1)</sup>. Based on the above, the missile equations of motion in wind axes are

$$\dot{V} = \frac{T}{m} \cos \alpha \cos \beta - g \sin \gamma - \frac{D}{m} \tag{1}$$

$$\dot{\chi} = \frac{1}{mV \cos \gamma} (-T \cos \alpha \sin \beta + Y) \tag{2}$$

$$\dot{\gamma} = \frac{T}{mV} \sin \alpha - \frac{g}{V} \cos \gamma + \frac{L}{mV} \tag{3}$$

where the symbols follow the standard nomenclature. To improve the numerical stiffness of the algorithm during the optimization, the system (1)-(3) is made nondimensional defining the parameters:

$$\tau = \frac{g}{a} t \quad \text{nondimensional time} \tag{4}$$

$$T_w = \frac{T}{mg} \quad \text{Thrust/Weight ratio} \quad (5)$$

$$S_w = \frac{\rho a^2 S}{2mg} \quad \text{nondimensional reference area} \quad (6)$$

$$M = \frac{V}{a} \quad \text{Mach number} \quad (7)$$

Indicating the nondimensional time derivative as  $(\cdot)' = d/d\tau$ , the equations of motion become

$$M' = T_w \cos \alpha \cos \beta - \sin \gamma - S_w M^2 C_D \quad (1)$$

$$\chi' = \frac{1}{\cos \gamma} \left( -\frac{T_w}{M} \cos \alpha \sin \beta + S_w M C_Y \right) \quad (2)$$

$$\gamma' = \frac{1}{M} (T_w \sin \alpha - \cos \gamma) + S_w M C_L \quad (3)$$

The nondimensional kinematic equations are then given by

$$X' = M \cos \gamma \cos \chi \quad (8)$$

$$Y' = M \cos \gamma \sin \chi \quad (9)$$

$$Z' = -M \sin \gamma \quad (10)$$

The basic data for the specific missile are taken from<sup>(1)</sup> and will not be repeated here:

### Missile Aerodynamics

The missile aerodynamic properties are one of the major issues whenever dynamics and control problems are addressed. The absence of experimental data is particularly critical in the present study, since flight mechanical characteristics at high angles of attack are analyzed. To this point, the only available source of information for the authors is represented by Ref. 1, where a prediction of lift  $C_L(\alpha, M)$  and drag  $C_D(\alpha, M)$  coefficients was presented, limited to the longitudinal plane and based on Missile DATCOM<sup>(2)</sup> software up to the assumed stall value and classical fluidynamics prediction formulas at high angles of attack<sup>(3)</sup>. For the present problem, we assume a functional relationship for the aerodynamic coefficients of the form  $C_i = C_i(\alpha, \beta, M)$ , with  $i = L, D, Y$ . The coefficients are extrapolated from the estimated values available in Ref. (1) and assuming a symmetric behavior with respect to the missile principal axis. Under the above assumptions, the effective angle of attack is computed first as

$$\alpha_{eff} = \cos^{-1}(\cos \alpha \cos \beta) \quad (11)$$

based on the values of  $\alpha_{eff}$  and speed, we can compute  $C_D, C_{Leff}$  from Ref. (1). Lift and side force coefficients  $C_L$  and  $C_Y$  are then computed by projection of  $C_{Leff}$  on the yz wind axes plane, yielding

$$C_L = \frac{\sin \alpha C_{Leff}}{\sqrt{\cos^2 \alpha \sin^2 \beta + \sin^2 \alpha}} \quad (12)$$

$$C_Y = \frac{\cos \alpha \sin \beta C_{Leff}}{\sqrt{\cos^2 \alpha \sin^2 \beta + \sin^2 \alpha}} \quad (13)$$

Equations (12) and (13) are then saved in a look-up-table as functions of angle of attack and Mach number and made available to the optimization algorithm. Lift and drag curves are shown in figures 1 and 2 respectively.

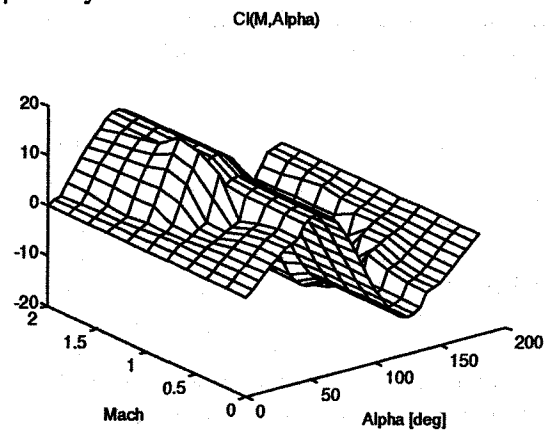


Figure 1. Effective Lift Coefficient

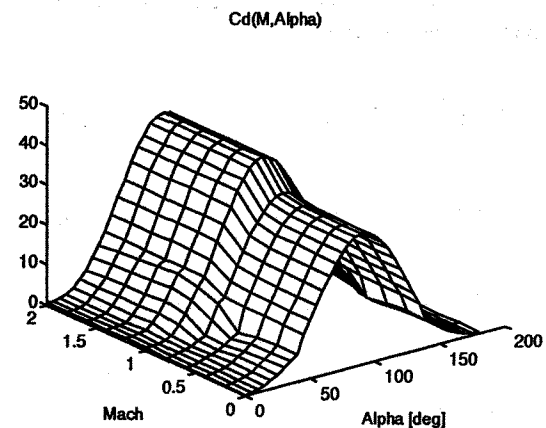


Figure 2. Drag Coefficient

The interpolation procedure is important for smoothing the data used by numerical algorithms such as any optimization method. Currently, a multilinear interpolation method is used, to guarantee the continuity of the aerodynamic coefficients, needed by

the gradient-based optimization. Improvement on the interpolation is underway, so that continuity of first and second derivatives of the coefficients is also ensured. The modification uses Q-patches proposed by Bless and Moerder<sup>(7)</sup>, characterized by quadratic and/or quartic functions in the proximity of the data points, which improve considerably the computational efficiency, especially during multi-dimensional interpolation. Convexity and monotonicity of the resulting composite functions are maintained imposing the cubic term to be zero.

### Finite Horizon Optimal Control Strategy

A discrete time optimal control approach will be used in the optimal trajectory computation<sup>(4)</sup>. The reason for this choice lies in the fact that the implementation of the guidance and autopilot systems will be probably digital and a direct discrete time approach appears more consistent at this point. The vehicle dynamics are then written in the following general form:

$$\underline{x}_{i+1} = \underline{f}_i(\underline{x}_i, \underline{u}_i) \quad (14)$$

which is nothing but a sequential set of equality constraints, where  $\underline{x}_i$  are the system's state variables corresponding to a sampling time  $i$  and  $\underline{u}_i$  are the inputs. All the variables need to be perfectly known and the absence of external disturbances is assumed, but this formulation is otherwise general since the system can be both nonlinear and time varying.

In order to execute an optimal N-step maneuver, a cost functional must be defined, and the solution consists on finding the sequence of  $N$  system inputs which minimizes the cost functional. A general form for the index of performance is given by

$$J = \sum_{i=0}^{N-1} h_i(\underline{x}_i, \underline{u}_i) + h_N(\underline{x}_N, \underline{u}_N) \quad (15)$$

where  $h_i(\underline{x}_i, \underline{u}_i)$  includes items such as tracking error, control variables cost, state and control constraints, etceteras, while  $h_N(\underline{x}_N, \underline{u}_N)$  takes into account possible constraints on the desired final state error. The expression of the performance index may be nonlinear, and the finite horizon optimization can be stated as follows:

*Given an initial state  $\underline{x}_0$ , find the succession of optimal controls  $\underline{U} = \{\underline{u}_0, \underline{u}_1, \dots, \underline{u}_{N-1}\}$  to be applied to (14) so that (15) is a minimum.*

In practice, a succession of open loop controls must be found so that the system can reach the desired final state with the minimum associated cost. Since the cost is expressed by (15), we can also write

$$J = J(\underline{x}_0, \underline{u}_0, \dots, \underline{u}_{N-1}) \quad (16)$$

The simplest numerical approach to solve the optimization stated by (14) and (15) is an iterative first order gradient-based descent of the cost functional yielding, at each step

$$\underline{U}(k+1) = \underline{U}(k) - \alpha \nabla_{\underline{U}} J[\underline{x}_0, \underline{U}(k)] \quad (17)$$

It can be shown that (17) can be calculated using the following algorithm:

$$\lambda_N^T = \frac{\partial h_N(\underline{x}_N)}{\partial \underline{x}_N} \quad (18)$$

$$\lambda_i^T = \frac{\partial h_i(\underline{x}_i, \underline{u}_i)}{\partial \underline{x}_i} + \lambda_{i+1}^T \frac{\partial \underline{f}_i(\underline{x}_i, \underline{u}_i)}{\partial \underline{x}_i} \quad (19)$$

$$\frac{\partial J}{\partial \underline{u}_i} = \frac{\partial h_i(\underline{x}_i, \underline{u}_i)}{\partial \underline{u}_i} + \lambda_{i+1}^T \frac{\partial \underline{f}_i(\underline{x}_i, \underline{u}_i)}{\partial \underline{u}_i} \quad (20)$$

with the gradient in (20) computed by calculating the derivatives of which it is composed, and  $\lambda_i$  the sequence of Lagrange multipliers defined as

$$\lambda_i^T = \frac{\partial J}{\partial \underline{x}_i}$$

As any first order gradient-based procedure, convergence to an absolute minimum is not guaranteed. A good initial guess, based on the physical knowledge of the problem, is always appropriate, coupled with a simulation campaign capable of indicating the feasibility of the solution. The discrete-time optimization, although strictly speaking less general than a continuous one, tends to the continuous optimal solution as the sampling time goes to zero. It has the advantage of a simpler algorithm (numerical solution is needed anyway even for continuous systems), which helps in reducing the possibility of the minimization yielding a local minimum. Of course, the problem of local minima can be always controlled, to a certain extent, by varying (reducing) the descent step  $\alpha$ , at the expenses of a slower convergence speed. The procedure described above is open loop at each step and it requires a closed loop structure in order to achieve optimality over the entire trajectory. This can be accomplished by a receding horizon technique<sup>(4)</sup> which consists of the following iterative steps:

*Step 1:* Given the  $i$ th state  $\underline{x}_i$  (and  $N$  reference values, if any), the succession of optimal controls to be applied

to (14)  $\underline{U}_i = \{\underline{u}_i, \underline{u}_{i+1}, \dots, \underline{u}_{i+N-1}\}$  must be sought so that (15) is minimum.

*Step 2:* Only  $\underline{u}_i$  is applied to the system, then  $\underline{x}_{i+1}$  is measured and  $\underline{U}_{i+1} = \{\underline{u}_{i+1}, \underline{u}_{i+2}, \dots, \underline{u}_{i+N}\}$  is computed. Note that  $\{\underline{u}_{i+1}, \underline{u}_{i+2}, \dots, \underline{u}_{i+N-1}\}$  have already been found in the previous step, so they can be employed to initialize the algorithm, making the current sequence optimization faster.

*Step 3:* The procedure is iterated over the entire trajectory.

The complete closed loop optimization procedure, for a  $S$ -step maneuver, is then composed of  $S$  open loop optimizations, but, in general, only the first one is critical so that an acceptable speed is generally retained. It must be noted that the approach is truly feedback in the sense that if a disturbance changes an optimal state  $\underline{x}_{i+1}$  to an incorrect value  $\underline{x}_{di+1}$ , the next sequence will provide compensation for the error.

#### Application

Since the optimization procedure needs a discrete time model of the process, the first step is to obtain a sampled data version of equations (1'), (2') and (3'). Because of the system's nonlinearity, classical equivalent models such as step (zero hold) invariant ones can not be used. A viable solution is using Euler's rule, that yields:

$$m(k+1) = m(k) + t_s \dot{m}(k) \quad (1'')$$

$$\chi(k+1) = \chi(k) + t_s \dot{\chi}(k) \quad (2'')$$

$$\gamma(k+1) = \gamma(k) + t_s \dot{\gamma}(k) \quad (3'')$$

The choice of the sampling time  $t_s$  is clearly important and must be a compromise between accuracy and computational speed. If we assume a maneuver of a duration of two to four seconds, a satisfactory starting choice for sampling time is 0.1 seconds.

At this point the controller structure relative to the maneuver of interest must be defined in more detail. The temporal window for the entire trajectory was chosen to be made up of 20-30 sequences. This choice, based on trial simulations, resulted in the best compromise between algorithm accuracy and speed. The performance index has three main components: tracking error, input cost penalty, and system's constraints leading to the form

$$h_i(\underline{x}_i, \underline{u}_i) = h_i^{x-err}(\underline{x}_i) + h_i^{u-cos}(\underline{u}_i) + h_i^{const}(\underline{x}_i, \underline{u}_i) \quad (21)$$

The components were selected as follows:

- A quadratic form for the state vector tracking error,

$$h_i^{x-err}(\underline{x}_i) = (\underline{x}_i - \underline{x}_i^{ref})^T P (\underline{x}_i - \underline{x}_i^{ref}) \quad (22)$$

where  $P$  is a positive definite diagonal weight matrix, whose elements specify the relative importance of the state variables. If all the states are equally important, the obvious choice for  $P$  is  $P = k_1 I$ , where  $k_1$  is a design parameter.

- A quadratic form for the control cost penalty:

$$h_i^{u-cos}(\underline{u}_i) = \underline{u}_i^T Q \underline{u}_i \quad (23)$$

where  $Q$  is diagonal, positive definite and furthermore  $\|Q\| \ll \|P\|$  and  $\|U\| \approx \|X\|$ , typically  $Q = k_2 I$  with  $k_2 \ll k_1$ . In other terms, the cost associated with the controls may be considered negligible (enough to avoid singular solution) in order to achieve a tracking as good as possible. A zero steady state error can not be obtained because no integral action is employed; however this is not fundamental for our purposes compared with the necessity of keeping the algorithm as simple as possible, in order to avoid local minima. The problem of appropriate constraints is critical to every optimization algorithm. In our case, the angle of attack is not limited by stall values, however it can not be arbitrarily large and a constraint is introduced. The constrained angle is neither  $\alpha$  nor  $\beta$ , but the trigonometric combination defined as effective angle of incidence  $\alpha_{eff}$ . Several different values for the maximum  $\alpha_{eff}$  were tried, and shown in the simulation results section.

The control variables can not have an instantaneous variation because of the actuators dynamics, thus a term penalizing abrupt variations is introduced. Usually such a constraint applies to the angles only. Finally, the thrust is assumed to be limited to 22 times the body weight. The constraints are introduced in the performance index by the terms

$$h_i^{const}(\underline{x}_i, \underline{u}_i) = \gamma(\underline{u}_i, \underline{u}_{i-1}) + \phi(\alpha_{eff}) + \varphi(T) \quad (24)$$

where

$$\gamma(\underline{u}_i, \underline{u}_{i-1}) = (\underline{u}_i - \underline{u}_{i-1})^T R (\underline{u}_i - \underline{u}_{i-1}) + (\Delta \underline{u}_i - \Delta \underline{u}_{i,max})^T S (\Delta \underline{u}_i - \Delta \underline{u}_{i,max}) \quad (24')$$

with  $\|S\| \gg \|P\| \approx \|R\|$  and  $\Delta u_i = |u_i - u_{i-1}|$ . The first term on the RHS of (24') is a soft constraint on the control, whereas the second term acts as hard limit. And

$$\phi(\alpha_{eff}) = s(\alpha_{eff} - \alpha_{maxeff})^2 h(\alpha_{eff} - \alpha_{maxeff}) \quad (25)$$

$$\varphi(T) = t(T - 22)^2 h(T - 22) \quad (26)$$

where  $h(\cdot)$  is the Heaviside function and  $R$  must be comparable with  $P$ , while  $s$  and  $t$  must be much larger in norm than the matrices mentioned above.

Although time of flight is not explicitly introduced in the cost function, the constraints that are introduced guarantee a behavior leading indirectly to a minimum time, while maintaining the missile physical integrity and characteristics.

### Preliminary Simulation Results

Several simulations were performed using the model defined by equations (1''), (2'') and (3'') and the optimal control algorithm of (18), (19) and (20). The main purpose of the test being, at this point, the evaluation of the algorithm and not the optimal selection. The results are shown next for a horizontal trajectory. All the simulations were performed using the following weighing matrices:  $P = 10I_3$ ,  $Q = k_2 I_3$  and  $k_2 = (0.01 - 0.1)$ ,  $R = \text{diag}\{100, 100, 0\}$ , and  $S = 10,000 * \text{diag}\{1, 1, 0\}$ .

The missile is required to execute a turn which lies approximately on the horizontal plane, with yaw and heading angles going from zero to 180°, while the reference pitch angle is set equal to zero. The initial and final velocities are constrained to be equal to Mach 0.8. Note that although their final values are fixed, speed and the pitch angle are permitted to vary during the curve if this can endorse the maneuver.

The optimization was performed for three different values of maximum sideslip angle, 40°, 80° and 120° respectively, while the limits on the maximum effective angle of attack in (25) were set to 34.3, 68.8, and 103.2 degrees respectively.

One curve, characterized by the lowest limit on the sideslip angle shows clearly a marked three-dimensional behavior compared to the other two. For the turn to be accomplished, with the constraint on the final speed, the missile tries to maintain a higher effective angle of attack and energy level. This curve is similar to a conventional turn, with the thrust level near the maximum at every instant. As the constraints on beta are relaxed, the higher heading rate allows for quicker turns, almost two-dimensional, with lower and more effective thrust expenditure. The next 3 figures

show the same trajectories, with their projections onto the 3 reference planes.

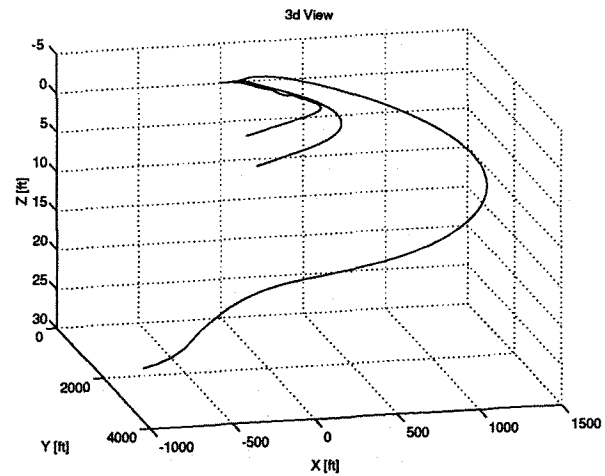


Figure 3. Horizontal Trajectories in 3D

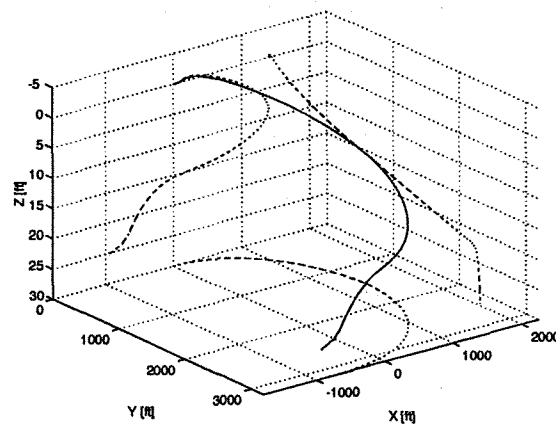


Figure 4. Trajectory for  $\beta_{max} = 40$  deg

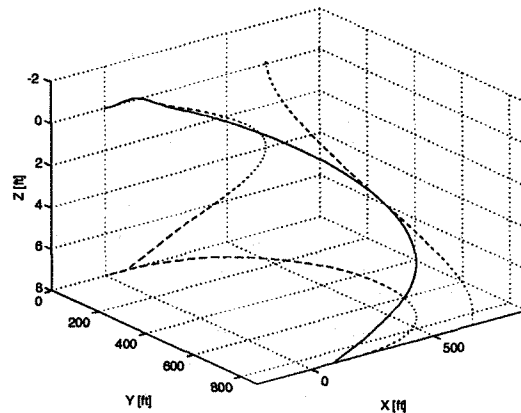


Figure 5. Trajectory for  $\beta_{max} = 80$  deg

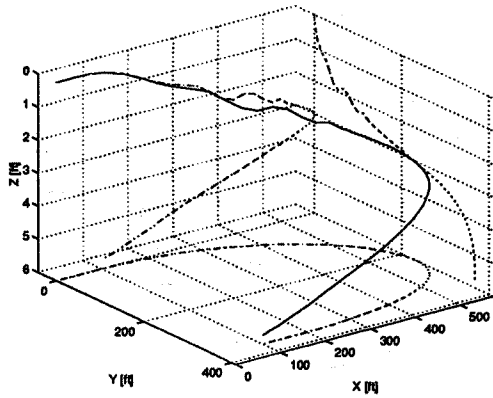


Figure 6. Trajectory for  $\beta_{max} = 120$  deg

The time history of heading, yaw, and sideslip angles are shown next for the 3 trajectories. Note that yaw angle behavior presents discontinuity due to the plotting set up.

The figures include the nondimensional thrust profile as well. Figure 10 shows the missile behavior superimposed to the trajectory, during the curve at the highest sideslip level. In this figure, a qualitative relationship among the angular variations can be seen, as well as the "post-stall" characteristics of the flight.

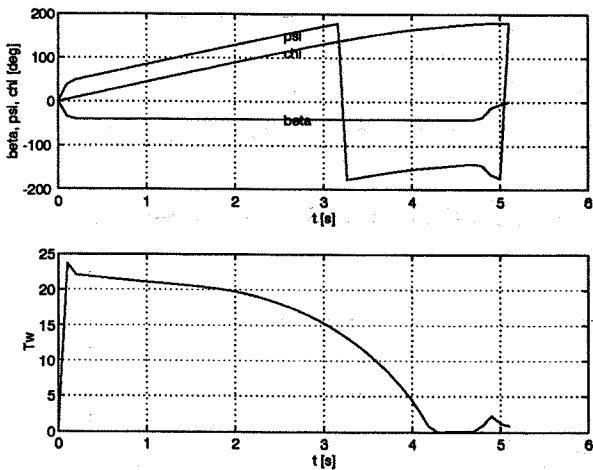


Figure 7. Angles Time Histories  $\beta_{max} = 40$  deg

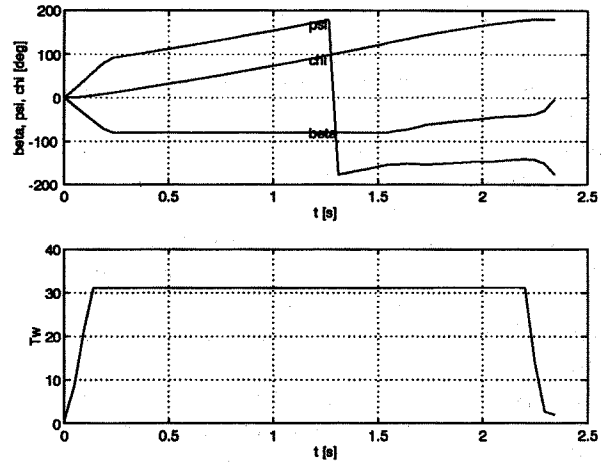


Figure 8. Angles Time Histories  $\beta_{max} = 80$  deg

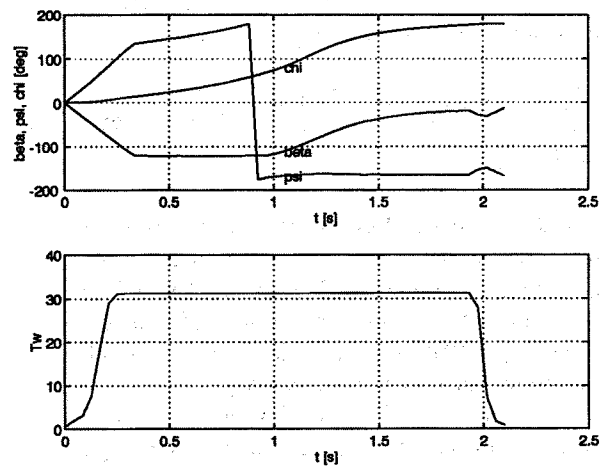


Figure 9. Angles Time Histories  $\beta_{max} = 120$  deg

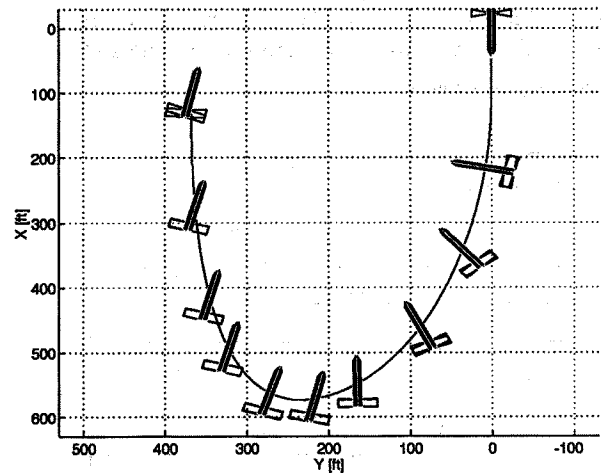


Figure 10. Graphical Representation of Missile Motion

### Differential Geometry Approach

Differential geometry is used in this work as a tool to investigate the agility characteristics of a particular

maneuver<sup>(5)</sup>. Agility has been widely studied in recent years as one of the components leading to the superiority of combat aircraft over the threat and defined as operational agility in a larger sense to encompass the entire weapon system.. Although airframe agility has been measured through simulation and, more recently, in flight testing, it still lacks a unified analytical background. A general agreement has been found among manufacturing, procuring and research agencies in that airframe agility is now associated with the rate of change of the maneuver plane and, as such, it has been recognized as a property of the flight path. The development of the governing equations is done using a differential geometry approach<sup>(6)</sup>, and the main elements needed to describe the flight path in a three dimensional space are the curvilinear coordinates. From Ref. 5, one definition of agility is the total time derivative of the acceleration vector measured in the Frenet trajectory frame

$$A = \dot{\underline{a}} = \left[ \ddot{s} - \dot{s}^2 \kappa^2 \right] \underline{t} + \left[ 3\dot{s}\dot{s}\kappa + \dot{s}^2 \dot{\kappa} \right] \underline{n} + \left[ \dot{s}^3 \kappa \tau \right] \underline{b} = \quad (27)$$

$$A_A \underline{t} + A_C \underline{n} + A_T \underline{b}$$

where  $\kappa$  and  $\tau$  are defined as curvature and torsion of the path, and the unit vectors in (27) identify the tangent, normal and binormal directions. The agility of the curve is then characterized by the value of the components in the RHS of (27), which represent axial, curvature and torsional agility respectively. For the maneuver at 120 deg. sideslip, Figures 11 and 12 show curvature and torsion for the low and high sideslip turns. The agility components defined also as "jerk vector" are shown for the same trajectories in figures 13 and 14. Although at the analysis level at this point, the behavior in the figures below is indicative of the increased maneuvering capabilities of the vehicle as  $\beta$  increases.

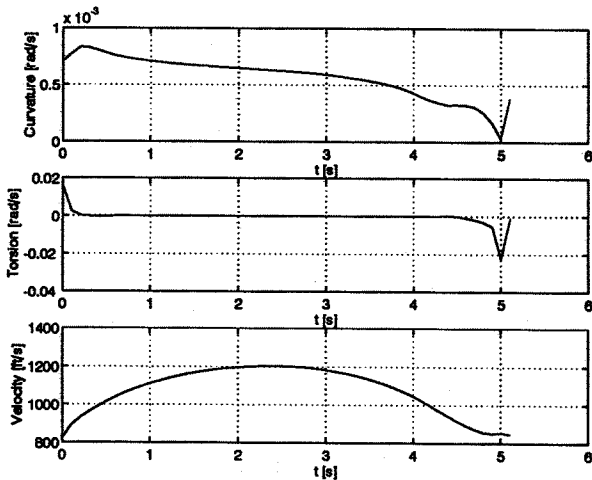


Figure 11. Curvature, Torsion and Speed ( $\beta_{max}=40$  deg)

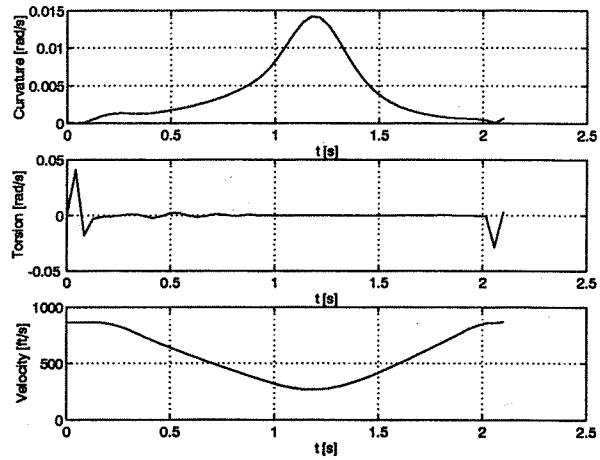


Figure 12. Curvature, Torsion and Speed ( $\beta_{max}=120$  deg)

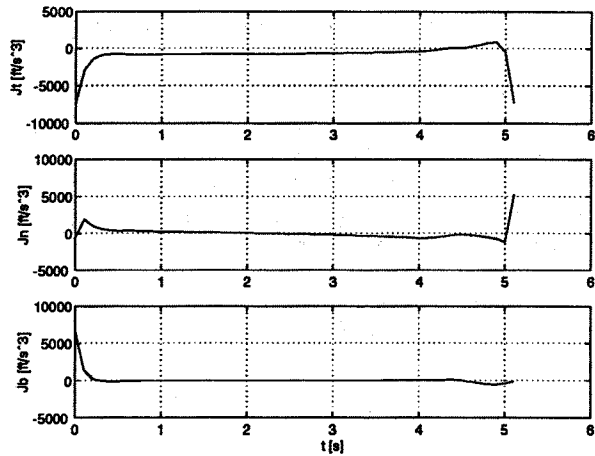


Figure 13. Agility Components Speed ( $\beta_{max}=40$  deg)

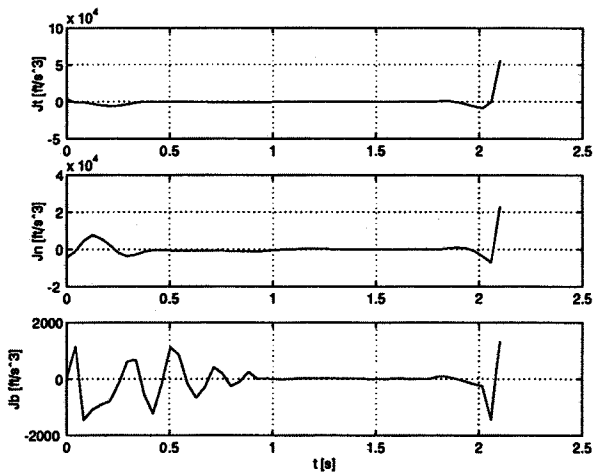


Figure 14. Agility Components Speed ( $\beta_{max}=120$  deg)

### Current Research

Work is being currently carried out in all the aspects mentioned in the paper.

In the area of optimization, the multistage algorithm is undergoing further development and comparison is being done with other techniques available in the literature such as direct shooting methods and quadratic programming. Once reliability and speed are evaluated, the use of fuzzy theory will be investigated as a tool for on-line porting. A comprehensive simulation campaign is being carried out to define sets of optimal trajectories in space. In addition, several flight vehicle parameters are currently changed (such as thrust/weight ratio, maximum aerodynamic angles, speed and time constraints at the boundaries) for sensitivity studies and preliminary design assessment. The equations of motion are currently being extended to include motion in the roll axis. This added degree of freedom will allow the simulation of "true" spatial trajectories. If aerodynamic data is made available, the attitude equations will be incorporated in the model as well.

The activity in agility is proceeding parallel to the above studies. It is expected that agility properties of optimal trajectories will be evaluated, and that an optimization based on agility equations and agility parameters in the performance index will be carried out in the near future.

### Acknowledgment

This work was sponsored by Wright Laboratory, WL/MNAV, Air Force Material Command, USAF, under Grant F08630-94-0001, the technical monitor was Mr. Federick A. Davis.

### References

- [1] Thukral, A., Cochran, J.E., Jr., "Evaluation of Variable Structure Control for Missile Autopilots using Reaction Jets and Aerodynamic Control", Final Report, Grant RDL-93-132, Auburn University, Alabama, May 1994.
- [2] Bruns, K.D., and others, "Missile DATCOM", WL-TR-91-3039.
- [3] Hoerner, S., "Practical Information on Fluid Dynamic Drag", Wiley 1958.
- [4] Bryson, A., Ho, Y. C., "Applied Optimal Control", Hemisphere, New York, 1975.
- [5] North Atlantic Treaty Organization: AGARD-AR-314, "Operational Agility", Technical Report of Working Group FMP19, 1994.
- [6] Miele, A. "Theory of Flight Paths", A. Wesley, 1962.
- [7] Bless, R.R., Moerder, D.D., "Computationally Efficient Method for Multidimensional Data

Interpolation", AIAA Guidance, Navigation and Control Conference, Baltimore, MD, August 1995.